THE ASTROPHYSICAL JOURNAL, 518:24–31, 1999 June 10

MEASURING THE COSMOLOGICAL GEOMETRY FROM THE Lyα FOREST ALONG PARALLEL LINES OF SIGHT

PATRICK MCDONALD AND JORDI MIRALDA-ESCUDÉ[1]
Department of Physics and Astronomy, University of Pennsylvania, Philadelphia, PA 19104
Received 1998 July 13; accepted 1999 January 19

ABSTRACT

The possibility of measuring the cosmological geometry using the redshift space correlation function of the Lyα forest in multiple lines of sight as a function of angular and velocity separation is discussed. The geometric parameter to be measured is $f(z) \equiv c^{-1}H(z)D_A(z)$, where $H(z)$ is the Hubble constant and $D_A(z)$ the angular diameter distance at redshift z. The correlation function is computed in linear theory, assuming that the Lyα forest is a result of gravitational instability in a photoionized intergalactic medium. We describe a method to measure the correlation from observations with the Gaussianization procedure of Croft et al. to map the observed Lyα forest transmitted flux to an approximation of the linear density field. The effect of peculiar velocities on the *shape* of the recovered power spectrum is pointed out. We estimate the error in recovering the $f(z)$ factor from observations due to the variance in the Lyα absorbers. We show that at least ~ 25 pairs of quasars (separations $<3'$) are needed to distinguish a flat $\Omega_0 = 1$ universe from a universe with $\Omega_0 = 0.2$, $\Omega_\Lambda = 0.8$. A second parameter that is obtained from the correlation function of the Lyα forest is $\beta \simeq \Omega(z)^{0.6}/b$ (affecting the magnitude of the peculiar velocities), where b is a linear theory bias of the Lyα forest. In the theory of the Lyα forest assumed here, the parameter β can be predicted from numerical simulations; once β is known, the number of quasar pairs needed to constrain f is reduced to about six. On small scales, where the correlation function is higher, $f(z)$ should be measurable with fewer quasars, but nonlinear effects must then be taken into account. The anisotropy of the nonlinear redshift space correlation function as a function of scale should also provide a precise quantitative test of the gravitational instability theory of the Lyα forest.

Subject headings: cosmology: theory — intergalactic medium — large-scale structure of universe — quasars: absorption lines

1. INTRODUCTION

One of the methods of measuring the parameters of the global cosmological metric of the universe is to observe the angular size and redshift extent of a set of objects, which can be assumed to be spherically symmetric and to follow the Hubble expansion on average (Alcock & Paczyński 1979). More generally, this geometric factor can be measured from a correlation function of any set of objects depending on angular separation and redshift difference, by requiring that the correlation be isotropic. It has long been known that this measurement at high redshift is sensitive primarily to the cosmological constant (Alcock & Paczyński 1979). The power of this method rests on the fact that no assumption of standard candles or rods is required, and it is therefore independent of evolutionary effects of the observed objects. However, generally the large-scale correlation of objects in the universe is induced by gravitational collapse, and the peculiar velocities make the correlation function in redshift space anisotropic (Kaiser 1987). The effect of peculiar velocities must be taken into account before the method can be applied.

Recently, a method has been developed to recover the power spectrum of mass fluctuations from quasar absorption spectra by measuring the one-dimensional power spectrum and converting it to the desired three-dimensional power spectrum (Croft et al. 1998, hereafter CWKH). This method suffers from peculiar velocity distortions similar to those that distort the isotropy of the correlation in redshift space. Here we consider the accuracy in the measurement of the redshift space correlation function from the Lyα forest in nearby pairs of quasars. We show that it is possible to disentangle the effects of geometry and peculiar velocities and recover the power spectrum of mass fluctuations from the correlations in the Lyα forest. We also demonstrate that the peculiar velocities are important for correctly deriving the shape of the power spectrum.

The calculations of this paper assume that the Lyα forest originates in gravitational collapse of a photoionized intergalactic medium (IGM) and that it is not significantly perturbed by other effects, such as powerful galactic winds producing shock heating in the IGM. In this theory, the observed fluctuations in optical depth closely track continuous fluctuations in the underlying mass density, instead of coming from a population of discrete absorbers. The widths of absorption lines are determined mostly by Hubble expansion as opposed to temperature broadening. Predictions for this theory can be obtained from hydrodynamic numerical simulations for the various models of structure formation, and they are found to be in fair agreement with observations (e.g., Rauch et al. 1997; Theuns et al. 1998 and references therein). The theory is also supported by observations of quasar pairs, where structures are found to be correlated on comoving scales of hundreds of kiloparsecs and smooth on scales that are much smaller (e.g., Bechtold et al. 1994; Dinshaw et al. 1994; Fang et al. 1996; Crotts & Fang 1998; D'Odorico et al. 1998).

In § 2 we summarize the equations describing the cosmological geometry, discuss the linear theory correlation function in redshift space, and comment about the effect of

[1] Alfred P. Sloan Fellow.

peculiar velocities on the shape of the power spectrum. In § 3 we use a random line model to estimate the error in the measurement of $f(z)$ from a given number of observed quasar spectra. The discussion is given in § 4. Figures 6–9 contain the main results of this paper.

2. LINEAR THEORY OF THE Lyα FOREST CORRELATION FUNCTION

2.1. *Cosmological Geometry*

The following is a short summary of the cosmological equations we will use (these have been discussed earlier in several papers, e.g., Matsubara & Suto 1996; Ballinger, Peacock, & Heavens 1997). Observations directly measure the angular and redshift position of each object. We write the angular and redshift separation between two objects as $(\Delta z, \Delta\theta)$. The redshift is caused both by Hubble flow velocities (v_h) and peculiar velocities along the line of sight (v_p). The total velocity separation along the line of sight is $\Delta v_{\|} = c\,\Delta z/(1+z) = \Delta v_h + \Delta v_p$. It is also convenient to define a perpendicular velocity separation, $\Delta v_{\perp} = cf(z)\Delta\theta$, where $f(z)$ is a dimensionless function of redshift that includes all the dependence on the global cosmological metric. With the assumption of isotropy, the real space two-point correlation function of density fluctuations $\xi_r(\Delta v_h, \Delta v_{\perp})$ must be a function of $(\Delta v_h^2 + \Delta v_{\perp}^2)^{1/2}$ only. If ξ_r could be measured, it would be a relatively straightforward matter to measure $f(z)$ by simply demanding isotropy. In reality, distances cannot be measured accurately, and only the redshift space correlation function ξ, which is affected by peculiar velocities, can be determined. The peculiar velocities introduce an anisotropy in ξ of the same order as the difference in $f(z)$ between various cosmological models.

The quantity $f(z) \equiv \Delta v_{\perp}/(c\,\Delta\theta) = c^{-1}H(z)D_A(z)$ is simply the conversion factor between observed angular separation at redshift z and the corresponding Hubble velocity separation perpendicular to the line of sight. In the range of redshifts of interest for Lyα forest observations, $f(z)$ depends primarily on the cosmological constant (or other negative pressure components), being smaller compared with the Einstein–de Sitter model. The reason is that the Hubble constant $H(z)$ at high redshift is smaller in models where the expansion rate is being accelerated at present. This decrease in the Hubble constant is greater than the increase in the angular diameter distance, causing a net decrease in the value of $f(z)$. In the case of open models, the decrease of $H(z)$ and increase of $D_A(z)$ almost cancel each other, so $f(z)$ is rather insensitive to space curvature.

The function $f(z)$ is predicted for any cosmological model. If the present density of matter (in units of the critical density) is Ω_0, and considering also a negative pressure component with density Ω_Λ and equation of state $p = w\rho$ (the case $w = -1$ is the cosmological constant), we have, for an open universe,

$$f(z) = \frac{E(z)\,\sinh\,\{\sqrt{\Omega_R}\int_0^z [dz/E(z)]\}}{(1+z)\sqrt{\Omega_R}}\,, \tag{1}$$

and for a flat universe,

$$f(z) = \frac{E(z)\int_0^z [dz/E(z)]}{(1+z)}\,. \tag{2}$$

Here $\Omega_R = 1 - \Omega_0 - \Omega_\Lambda$ ($\Omega_R = 0$ for a flat universe), and

$$E(z) = \sqrt{\Omega_0(1+z)^3 + \Omega_R(1+z)^2 + \Omega_\Lambda(1+z)^{3(1+w)}}\,. \tag{3}$$

Figure 1 shows the value of $f(z)$ for several illustrative models. Clearly $f(z)$ depends most strongly on Ω_Λ at all redshifts; for $z \sim 3$, the dependence on space curvature is especially small. The fractional difference between a cosmological constant universe and an Einstein–de Sitter universe is maximum around $z \sim 1$ but does not decrease significantly from the maximum at higher redshift. In models with $0 > w > -1$, $f(z)$ keeps decreasing relative to the Einstein–de Sitter model up to a higher redshift; thus, at $z = 4$, models with $\Omega_0 = 0.4$ have a lower value of $f(z)$ for $w = -\frac{2}{3}$ than for the pure cosmological constant case $w = -1$. Aside from measuring cosmological parameters, simply measuring $f(z)$ at high redshift would test the correctness of currently studied FRW cosmological models in a qualitatively novel regime.

2.2. *The Correlation Function in Redshift Space*

In linear theory, the redshift space correlation function of the density field is given by (Kaiser 1987; Lilje & Efstathiou 1989; Hamilton 1992; Fisher 1995)

$$\begin{aligned}\xi(\Delta v_{\|}, \Delta v_{\perp}) = (1 + \tfrac{2}{3}\,\beta + \tfrac{1}{5}\,\beta^2)\xi_0(s) \\ - (\tfrac{4}{3}\,\beta + \tfrac{4}{7}\,\beta^2)\xi_2(s)P_2(\mu) \\ + (\tfrac{8}{35}\,\beta^2)\xi_4(s)P_4(\mu)\,,\end{aligned} \tag{4}$$

where $s = (\Delta v_{\|}^2 + \Delta v_{\perp}^2)^{1/2}$, $\mu = \Delta v_{\|}/s$, $P_l(\mu)$ are the usual Legendre polynomials, and

$$\xi_l(s) = \frac{b^2}{2\pi^2}\int_0^{\infty} dk\,k^2 P(k) j_l\left[\frac{ks(1+z)}{H(z)}\right]. \tag{5}$$

The functions $j_l(x)$ are the usual spherical Bessel functions, and $P(k)$ is the power spectrum of the mass fluctuations. The parameter β is related to the linear theory bias b by $\beta = b^{-1}H(z)^{-1}(dD/dt)/D$, where D is the linear growth factor, $H(z)$ is the Hubble constant, and t is the age of the universe [see Peebles 1993; $H(z)^{-1}(dD/dt)/D \simeq \Omega(z)^{0.6}$ is a good approximation in most models].

Equation (4) is valid only in linear theory, and the correlation function ξ could only be determined directly from observations if the linear density field, δ, were known. Only the fraction of the flux that is transmitted, F, can be determined along a line of sight from the Lyα forest spectrum in a quasar (we assume here that the quasar continuum has been fitted to a model, allowing the transmitted flux fraction F to be measured at every pixel). We need a way to recover the linear density field δ from the observed F. In general, this cannot be done exactly, since F is only known along a line of sight, and the chaotic nature of nonlinear evolution limits the accuracy to which δ can be recovered. Here we adopt the Gaussianization procedure of CWKH (see also Weinberg 1992). Gaussianization assumes that the initial mass density fluctuations were Gaussian random and that evolution approximately preserves the rank order of densities even as it distorts the distribution from a Gaussian curve. In the case of the Lyα forest, values of the observed flux decrement are mapped monotonically onto a new variable δ required to have the probability distribution function

$$P(\delta) = \frac{1}{\sqrt{2\pi\xi(0)}}\,\exp\left[-\frac{1}{2}\,\frac{\delta^2}{\xi(0)}\right]. \tag{6}$$

Of course, the fluctuation amplitude $[\xi(0)]^{1/2}$ is not recovered by the assumption that the rank order is preserved. Computing the correlation function of the Gaussianized spectrum yields only the ratio $\tilde{\xi}(\Delta v, \Delta\theta) \equiv \xi(\Delta v, \Delta\theta)/\xi(0)$.

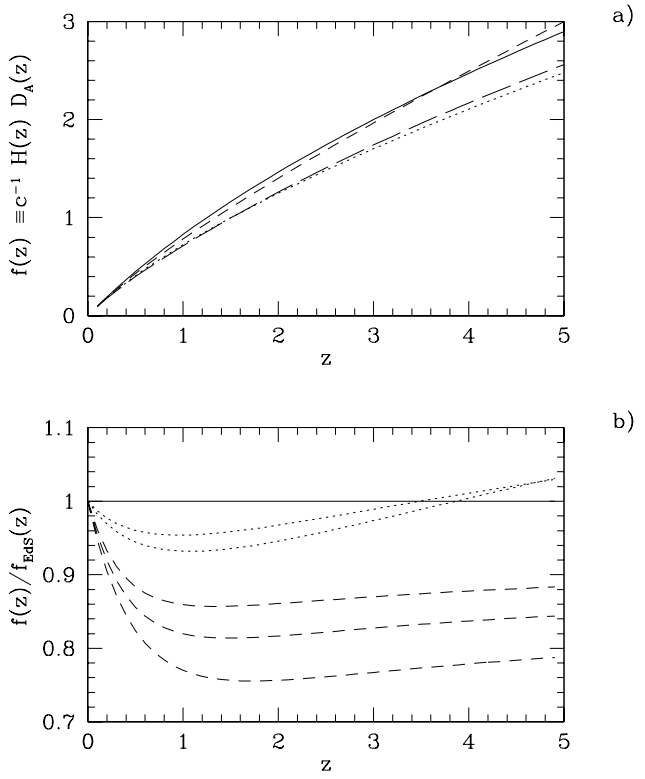

FIG. 1.—Scale factor relating angular separation to velocity separation for various cosmological models. (*a*) The function $f(z) \equiv \Delta v_\perp/(c\Delta\theta) = c^{-1}H(z)D_A(z)$ computed for $\Omega_0 = 1.0$, $\Omega_\Lambda = 0.0$ (*solid line*), $\Omega_0 = 0.4$, $\Omega_\Lambda = 0.6$, $w = -1$ (*long-dashed line*), $\Omega_0 = 0.3$, $\Omega_\Lambda = 0.0$ (*short-dashed line*), and $\Omega_0 = 0.4$, $\Omega_\Lambda = 0.6$, $w = -2/3$ (*dotted line*). (*b*) Ratio of $f(z)$ in various models to its value for $\Omega_0 = 1$, $\Omega_\Lambda = 0$. The dashed lines are flat models with $\Omega_\Lambda = 0.6$ (*top*), $\Omega_\Lambda = 0.7$ (*middle*), and $\Omega_\Lambda = 0.8$ (*bottom*). The dotted lines are $\Omega_\Lambda = 0$ models with $\Omega_0 = 0.4$ (*top*) and $\Omega_0 = 0.2$ (*bottom*). The value of $f(z)$ is highly sensitive to Ω_Λ primarily because models with a cosmological constant have smaller values of the Hubble constant at high redshift.

Once the new variable δ is obtained, the correlation function may be computed from observations through the usual estimator given by its definition: $\xi(\Delta\boldsymbol{v}) = \langle\delta(\boldsymbol{v})\delta(\boldsymbol{v}+\Delta\boldsymbol{v})\rangle$, where $\Delta\boldsymbol{v}$ symbolizes the vector separation $(\Delta v_\parallel, \Delta v_\perp)$. The average is taken over all pairs of pixels separated by $\Delta\boldsymbol{v}$ in the spectra available. However, this is not necessarily the best estimator of ξ, and in general it should be better to examine the full two-point joint probability distribution function. One of the main reasons for this is that the assumption that the density rank order is preserved should obviously break down at high optical depths, because the gas at high densities follows a highly stochastic evolution, and the observed spectrum is affected by multistreaming and thermal broadening. In addition, when $\tau \gg 1$ the value of δ derived from Gaussianization is subject to large errors arising from observational noise because of saturation. On the other hand, at low densities the evolution is not stochastic but regular even in the nonlinear regime, the optical depth is determined by a single stream, and thermal broadening can be neglected, so there should be a good correspondence between the optical depth at a given velocity and the gas density at the corresponding point in space.

The two-point distribution function for a Gaussian field is

$$P_2(\delta_1, \delta_2, \Delta\boldsymbol{v}) = \frac{1}{2\pi\sqrt{\xi(0)^2 - \xi(\Delta\boldsymbol{v})^2}} \times \exp\left[-\frac{1}{2}\frac{\xi(0)(\delta_1^2+\delta_2^2) - 2\delta_1\delta_2\xi(\Delta\boldsymbol{v})}{\xi(0)^2 - \xi(\Delta\boldsymbol{v})^2}\right]. \quad (7)$$

This can be rewritten as

$$P_2(\delta_1, \delta_2, \Delta\boldsymbol{v}) = P(\delta_1)\frac{1}{\sqrt{2\pi\xi(0)[1-\tilde{\xi}(\Delta\boldsymbol{v})^2]}} \times \exp\left\{-\frac{1}{2}\frac{[\delta_2 - \tilde{\xi}(\Delta\boldsymbol{v})\delta_1]^2}{\xi(0)[1-\tilde{\xi}(\Delta\boldsymbol{v})^2]}\right\}. \quad (8)$$

Thus for every value of δ_1 we can estimate $\tilde{\xi}(\Delta\boldsymbol{v})$ from the distribution of δ_2 conditional to the value of δ_1. For example, one could estimate $\tilde{\xi}(\Delta\boldsymbol{v})$ from the median of δ_2 (or any other adequate percentile) and see how the result depends on δ_1. Because the Gaussianized transmitted flux, δ, is actually not a Gaussian field owing to the nonlinear evolution, different statistical properties can be measured in addition to the usual correlation function defined as $\xi(\Delta\boldsymbol{v}) = \langle\delta(\boldsymbol{v})\delta(\boldsymbol{v}+\Delta\boldsymbol{v})\rangle$. For example, one can measure the median value of δ_2 under the condition that δ_1 is negative, as a function of $\Delta\boldsymbol{v}$; this can probably be obtained with greater precision than $\xi(\Delta\boldsymbol{v})$ owing to the problems mentioned above.

2.3. *The Effect of Peculiar Velocities on the Power Spectrum*

In their reconstruction of the linear power spectrum from Lyα forest lines, CWKH neglect the effect of peculiar velocities on the shape of $P(k)$. This effect arises in the conversion from the measured one-dimensional power spectrum P_{1D} to the desired three-dimensional power spectrum P_{3D}. While the shape of P_{3D} is not affected by peculiar velocities in linear theory (Kaiser 1987), P_{1D} *is* affected as shown by Kaiser & Peacock (1991):

$$P_{1D}(k_\parallel) = \frac{1}{2\pi}\int_{k_\parallel}^{\infty} dk\, k P_{3D}(k)\left(1+\beta\frac{k_\parallel^2}{k^2}\right)^2. \quad (9)$$

To demonstrate how this will affect the reconstruction of CWKH, we substitute a specific $P_{3D}(k)$ into equation (9), with various values of β. We use the cold dark matter power spectrum parameterization of Bardeen et al. (1986), with the coefficients of Ma (1996; see § 3.1 below), and the parameters $\Omega = 1$, $h = 0.5$, and $n = 1.0$. We then assume that the resulting P_{1D} is the one-dimensional power spectrum for the Lyα forest and attempt to reconstruct the three-dimensional power spectrum ignoring peculiar velocities (i.e., setting $\beta = 0$). This yields a new function $\tilde{P}_{3D}(k)$, different from the correct $P_{3D}(k)$ because of the effect of peculiar velocities, which is given by

$$\tilde{P}_{3D}(k) = P_{3D}(k)(1+\beta)^2 - \int_k^{\infty} dk'\left[\frac{4\beta}{k'}P_{3D}(k')\left(1+\beta\frac{k^2}{k'^2}\right)\right]. \quad (10)$$

The second term causes the change in the shape of $\tilde{P}_{3D}(k)$ relative to $P_{3D}(k)$. Figure 2 shows the results of this procedure for various values of β. The error in the reconstructed power spectrum grows with scale and eventually causes the results to become negative. The power spectrum

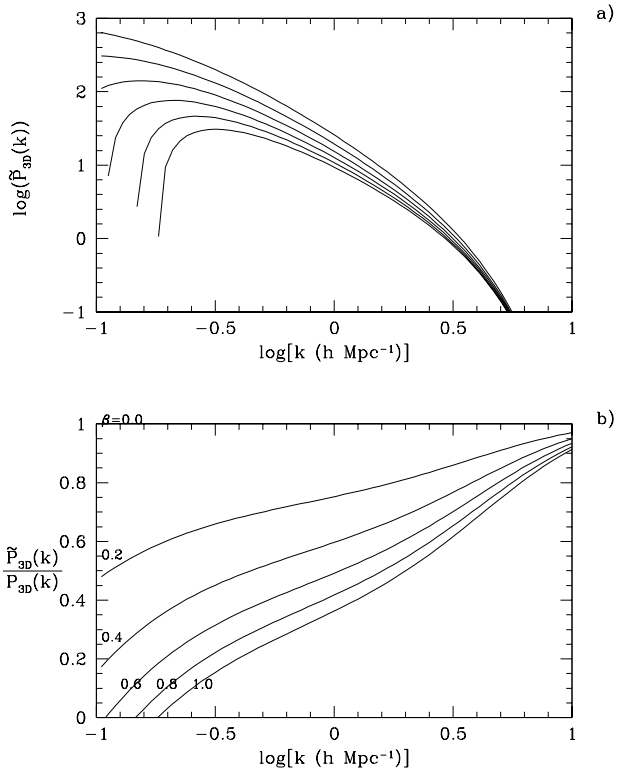

FIG. 2.—Demonstration of the error in the *shape* of a three-dimensional power spectrum if it is reconstructed from a one-dimensional power spectrum without considering the distortion caused by peculiar velocities. (*a*) The power spectrum as it would appear if reconstructed from $P_{1D}(k)$ while ignoring peculiar velocity effects. *Top to bottom*: $\beta = 0.0$, 0.2, 0.4, 0.6, 0.8, and 1.0. The $\beta = 0$ line yields the correct power spectrum. The normalization for all curves is fixed at large k, and a Gaussian cutoff has been applied. (*b*) The ratio of the reconstructed to the true power spectra. Ignoring peculiar velocities causes an underestimation of the large-scale power.

used in this figure was smoothed by a Gaussian function with radius $r_s = 0.24\ h^{-1}$ Mpc.[2] CWKH found that this was necessary to match the $P(k)$ they reconstructed from simulations.

Thus the shape of the mass power spectrum $P_{3D}(k)$ cannot be recovered until the parameter β is known. How can this parameter be determined? One could, in principle, attempt to determine β from observations in multiple lines of sight, as described in the next section. The anisotropy of the correlation function depends on the two parameters β and $f(z)$. But as we shall see, a very large amount of data will be required to measure both of them independently. If β can be predicted from theory, it should be much less difficult to determine the power spectrum and $f(z)$.

Linear theory would predict $b = 2$ for a constant temperature in the IGM, because the optical depth (which is the quantity that is modified by peculiar velocities in the mapping from real to redshift space) is proportional to the neutral hydrogen density or the square of the gas density. In a photoionized medium, the gas temperature is determined by a balance of photoionization heating and adiabatic cooling. The heating rate is proportional to the recombination rate, $\alpha\rho$, and the adiabatic cooling is proportional to the temperature T. Since $\alpha \propto T^{-0.7}$, the relation $T \propto \rho^{0.6}$ is set up if the gas temperature is not affected by shocks or reionization (see Hui & Gnedin 1997; Croft et al. 1997). This leads to a neutral hydrogen density proportional to $\alpha\rho^2 \propto \rho^{1.6}$ and therefore a Lyα forest bias $b = 1.6$. Since $\Omega(z) \simeq 1$ at $z \sim 3$ for viable models, $\beta \simeq 0.6$. However, in reality the bias depends on the relation of optical depth to the initial density on small scales, where nonlinearities are important, and therefore the correct bias to use in equations (6), (9), and (10), where linear theory is applied to large scales using the Gaussianization approximation, could be substantially different. Numerical simulations can be used to calculate a better value for the Lyα forest bias (which will in general depend on redshift), but of course this will only be accurate if the simulations are modeling the structure of the Lyα forest correctly.

The effects of peculiar velocities on the recovery of the mass power spectrum have independently been pointed out in a recent paper by Hui (1998), which appeared as this paper was being completed.

3. ERRORS IN THE MEASUREMENT OF THE Lyα FOREST CORRELATION

In this section, an estimate is obtained of the statistical error in measuring the parameters of the correlation function due to the random nature of the absorption lines that appear in the spectra. A simple model of absorption lines will be used to generate random spectra that reproduce the characteristics of the individual Lyα forest absorption lines without the large-scale correlation. We focus on the error induced by random fluctuations in the density field itself rather than the errors due to observational noise. The variance of the density field dominates the total error because the intrinsic variability of the Lyα forest is much larger than the observational noise in the high-quality spectra of quasars that can now be routinely obtained. Therefore, the measurement of $f(z)$ will be limited by the number of observed close pairs, and it does not require the highest quality spectra for the case of wide separations, when the differences between the two parallel spectra are large.

3.1. *Parameterization of the Correlation Function*

As discussed in § 2, two parameters describe the anisotropy of the correlation function: $f(z)$, reflecting the effect of the cosmological geometry, and $\beta(z)$, incorporating the peculiar velocity effects. We also parameterize the shape of the power spectrum to a fitting formula for cold dark matter models,

$$P(k_s) = \frac{k_s^n [\ln(1 + \alpha_1 q)/\alpha_1 q]^2}{[1 + \alpha_2 q + (\alpha_3 q)^2 + (\alpha_4 q)^3 + (\alpha_5 q)^4]^{1/2}}, \quad (11)$$

where $q \equiv k_s/\Gamma(z)$. We have reexpressed the power spectrum in terms of $k_s = k(1 + z)/H(z)$. The free parameters of this model for the shape of the power spectrum are n and $\Gamma(z)$ [given by $\Gamma(z) = (1 + z)\Omega_0 h^2/H(z)$]. The formula is given by Bardeen et al. (1986), but we modify the parameters to the fit for $\Omega_b = 0.05$: $\alpha_1 = 2.205$, $\alpha_2 = 4.05$, $\alpha_3 = 18.3$, $\alpha_4 = 8.725$, and $\alpha_5 = 8.0$ (Ma 1996). In addition, we include a smoothing parameter by multiplying the above formula by the factor $\exp(-k_s^2 v_s^2/2)$, with $v_s = r_s H(z)/(1 + z) = 48$ km s^{-1} at $z = 3$. This is motivated by the result of CWKH, who find that the Lyα forest has a power spectrum (after Gaussianization) that can be well approximated by a

[2] The value of r_s quoted in CWKH (in the caption of their Fig. 2) was wrong by a factor of 2π (R. A. C. Croft 1998, private communication).

smoothed version of the power spectrum of the mass. We fix v_s (rather than r_s) to the same value for all models, since the observations always yield separations in terms of velocity.

In Figure 3 we display the computed $\tilde{\xi}(\Delta v, \Delta\theta)$ along the line of sight ($\Delta\theta = 0$; *solid line*) and at separations $\Delta\theta = 127''$ and $\Delta\theta = 300''$ (*dashed lines*) at mean redshift $\langle z \rangle = 2.25$. Because of the Gaussianization, we measure $\tilde{\xi}(\Delta v, \Delta\theta) \equiv \xi(\Delta v, \Delta\theta)/\xi(0)$. The model parameters are $\Omega_0 = 1.0$, $\Omega_\Lambda = 0.0$, $h = 0.65$, $n = 1.0$, and $\beta = 0.6$. These parameters correspond to $f(z) = 1.61$ and $\Gamma(z) = 0.0036$ (km s^{-1})$^{-1}$. Also shown in the figure are the predictions for a model with $f(z) = 1.39$ (the value for $\Omega_0 = 0.4$, $\Omega_\Lambda = 0.6$), but with Γ, n, β, and v_s unchanged. The only effect of the value $f(z)$ predicted by different models is to set the scale for the transverse coordinate. The predicted correlation function for low f (e.g., for a Λ model) will be larger at the same angular separation than the prediction for the Einstein–de Sitter case, simply because the velocity separation for a given $\Delta\theta$ is smaller in the low-f model. Note that we are not discussing the expected change in the correlation function due to the different initial power spectra of the models. The change in the shape of the power spectrum in different models is a small effect, which can change the correlation function itself but does not significantly affect the accuracy in measuring the ratio of the correlation along and across the line of sight.

3.2. *Analysis of Random Spectra*

In this subsection we use a random line model to estimate the noise in the measurement of $\tilde{\xi}(\Delta v, \Delta\theta)$. We create Ly$\alpha$ forest spectra using a code that produces lines by randomly distributing Voigt profiles with a specified distribution of column densities N and widths b. Figure 4 shows a piece of one of these spectra. We take a set of parameters that closely match the distribution in the observations (e.g., Kim et al. 1997). We will consider the mean redshift $\langle z \rangle = 2.25$. We set the number of lines per unit redshift with column density greater than 10^{14} cm^{-2} to be $N_{>14} = 50$ and set $f(N) \propto N^{-1.35}$ with a break to $N^{-1.7}$ at log $N = 14.3$. We set the mean b-parameter of the Voigt profiles to be $\langle b \rangle = 30$ km s^{-1}, with a Gaussian dispersion of $\sigma_b = 12$ km s^{-1} and a lower cutoff of $b_{\rm cut} = 24$ km s^{-1}.

A spectrum is generated by calculating the transmitted flux at discrete pixels from the list of randomly generated lines. We then make a transformation of the transmitted flux to a new variable δ, requiring that the probability distribution of δ is Gaussian (this is the Gaussianization procedure). Because the absorption lines are random, there should be no correlation at separations beyond the width of the individual components, so any correlation we measure at larger separations is due to noise. Figure 5 shows the resulting $\tilde{\xi}(\Delta v, 0)$ for a pair of lines. The self-correlation of the individual components due to their own width extends out to $\Delta v \simeq 130$ km s^{-1}. The rms fluctuation around the mean $\tilde{\xi}$ is $\sigma_{\tilde{\xi}} \simeq 0.03$. The errors in ξ are obviously also correlated over ~ 100 km s^{-1} because of the width of the lines.

3.3. *Estimation of Errors*

We now estimate the errors in measuring parameters in the correlation function from a given set of quasar spectra. We consider first as an example the triplet of quasars of Crotts & Fang (1998), which have a useful redshift range $z \simeq 2.0$–2.5 and separations $\Delta\theta = 127''$, $147''$, and $177''$. The error bars we have computed for $\tilde{\xi}$ are not necessarily Gaussian and certainly not independent, so we use a Monte Carlo technique. We introduce noise to the calculated correlation function of a model by adding the noise values

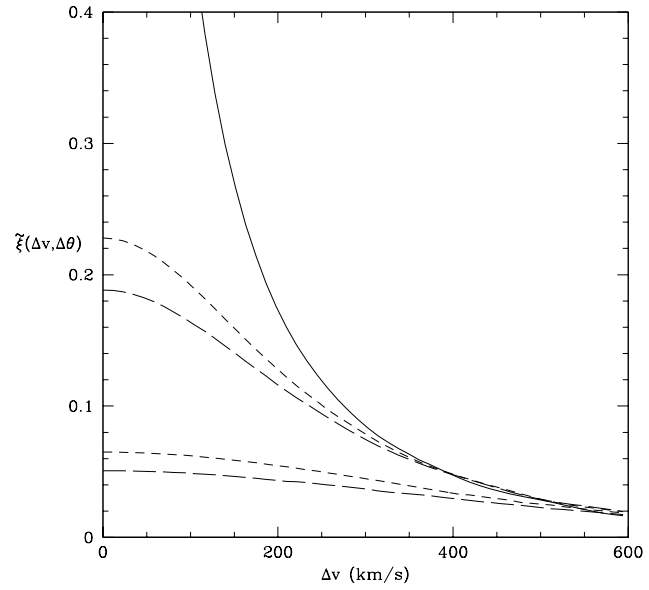

FIG. 3.—Linear theory predictions for the correlation function of the Gaussianized flux measured from quasar pairs. The solid and long-dashed lines are predictions for the correlation function for a flat model with $\Omega_0 = 1.0$, $h = 0.65$, and $\beta = 0.6$ [giving $f(z) = 1.61$]. The solid line is the correlation along the line of sight [normalized to $\tilde{\xi}(0, 0) = 1$]. The upper dashed lines are for $\Delta\theta = 127''$, and the lower dashed lines are for $\Delta\theta = 300''$. The short-dashed lines were produced by changing $f(z)$ to 1.39, appropriate for a flat $\Omega_\Lambda = 0.6$ model, *without* changing the power spectrum parameters or β (the line-of-sight correlation is the same in each case). The correlation at a given $\Delta\theta$ is larger in low-f models (e.g., models with Λ) because the implied transverse velocity separation in these models is smaller.

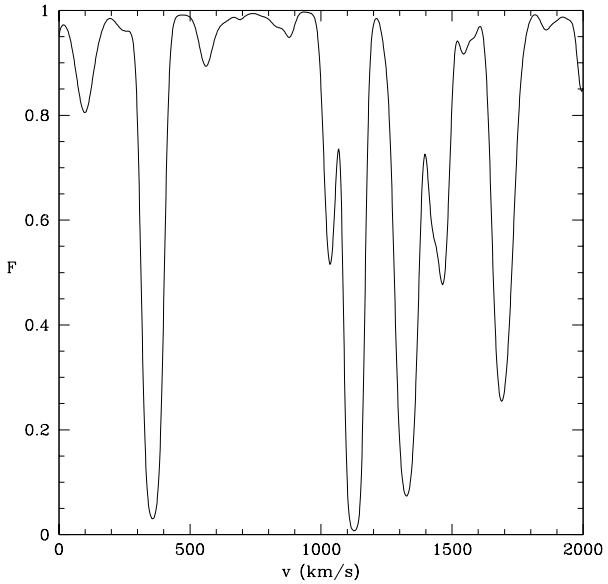

FIG. 4.—Flux vs. velocity for a randomly generated spectrum. The spectra are generated by randomly distributing a set of Voigt profiles with number density, column density distribution, and b-parameter distribution matching observational determinations. The spectra will be Gaussianized before their correlation function is measured.

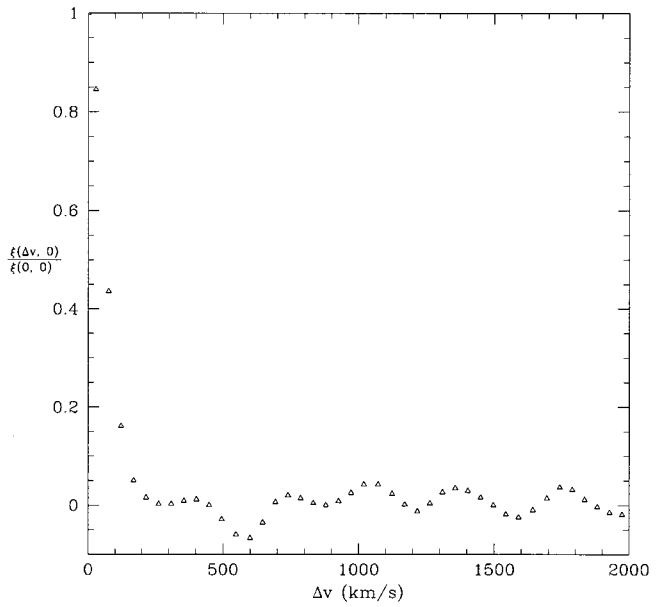

FIG. 5.—Example of the estimated correlation function from randomly generated, Gaussianized spectra, with a total redshift extent $\Delta z = 0.5$, at redshift $\langle z \rangle = 2.25$.

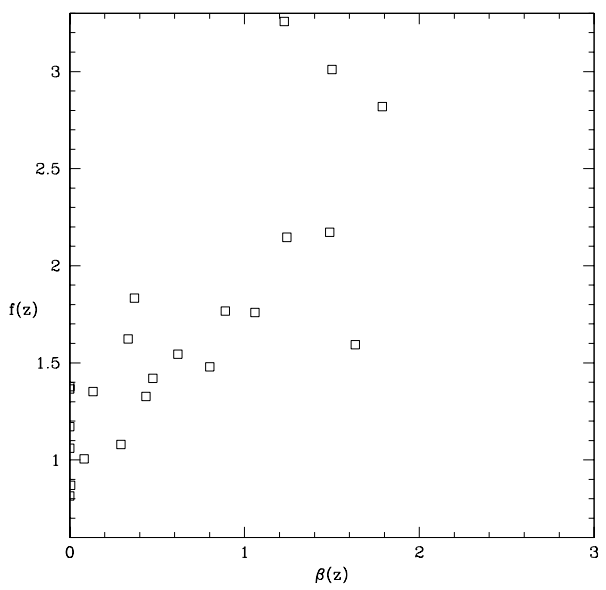

FIG. 6.—Expected scatter in measured parameters. Best-fit values for the parameters $\beta(z)$ and $f(z)$ are shown for 25 realizations of the spectra of a triplet of quasars with angular separations 127″, 147″, and 177″, with a useful redshift range $z = 2.0$–2.5. The true parameter values were $\beta(z) = 0.6$ and $f(z) = 1.61$. $f(z) = 1.61$ corresponds to $\Omega_0 = 1.0$ and $\Omega_\Lambda = 0.0$ at redshift $\langle z \rangle = 2.25$. Two points with high β do not appear on the plot. The constraint $\beta \geq 0$ was applied to the fits. Obviously the scatter is too large for an accurate distinction between cosmological models, which differ in f by typically $\sim 20\%$ (see Fig. 1).

of the correlation measured from spectra of randomly generated lines (i.e., we sum the curves in Figs. 3 and 5). We then fit the five parameters of the model, minimizing the χ^2 of the correlation function in linear bins of ~ 45 km s^{-1}, using the error bars found from the dispersion in the correlation obtained from the spectra of random lines. We repeat this procedure independently 25 times and fit each of the 25 simulated correlation functions separately. This should give the range of the fitted values we would expect to obtain from data with some fixed true parameter values. We do not use the correlation function at separations less than 300 km s^{-1}, approximately the scale of nonlinearities. Changing this restriction to 200 km s^{-1} results in a small improvement (particularly tighter correlation between f and β) but does not substantially change our conclusions. Figure 6 shows the results for the $f(z) = 1.61$, $\beta = 0.6$ model, fitted to the triplet of quasars described above. We will use this model for all our examples.

The results shown in Figure 6 indicate that the use of this triplet of quasars alone is insufficient to distinguish currently popular cosmological models. Figure 1 shows that the differences in f between models with and without a significant cosmological constant are typically $\sim 20\%$, while the scatter in measured values of f in Figure 6 is more than a factor of 2. A larger number of quasar pairs is needed to reduce the scatter. Figure 7 shows the improvement that can be expected by combining multiple pairs of quasars at different angular separations (but still at the same redshift). Six pairs with separations $\Delta\theta = 45''$, $75''$, $105''$, $135''$, $165''$, and $195''$ and with useful redshift range $z = 2.0$–2.5 are combined. The scatter in the results is still too large to allow a meaningful measurement of f. In Figure 8 we use the same six angular separations as in Figure 7 but reduce the noise in the correlation across the line of sight by a factor of 2 and reduce the noise in the line-of-sight correlation by a factor of 6. This noise reduction should be equivalent to considering 24 pairs of quasars, with an additional 384 single quasars included to improve the measurement of the line-of-sight correlation. Horizontal lines in the figure show the value of f for different values of Ω_Λ. With this many quasars, it is just becoming possible to distinguish an Einstein–de Sitter model from a flat model with $\Omega_\Lambda = 0.8$.

An independent determination of β, from theory or numerical simulations, can improve the accuracy of the

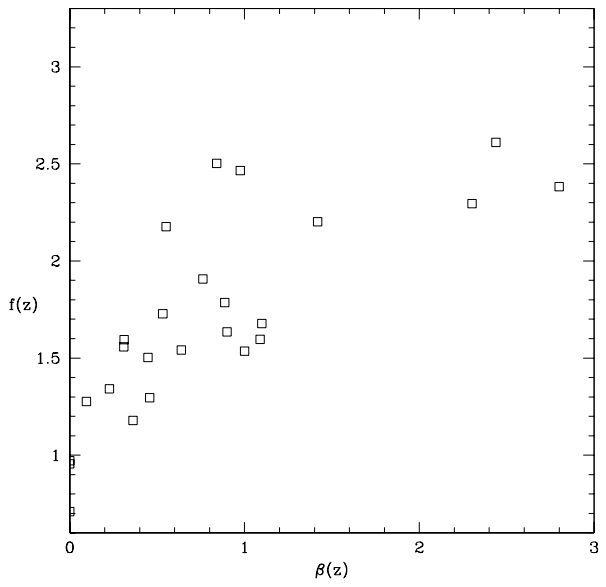

FIG. 7.—Scatter in measured parameters as in Fig. 6, with more quasars. Best-fit values of f and β are shown for 25 random realizations of six pairs of quasars separated by $\Delta\theta = 45''$, $75''$, $105''$, $135''$, $165''$, and $195''$. The true parameter values were $\beta(z) = 0.6$ and $f(z) = 1.6$ ($\Omega_0 = 1.0$, $\langle z \rangle = 2.25$). The constraint $\beta \geq 0$ was applied to the fits. While the scatter in f is noticeably decreased, it is still much too large to distinguish cosmological models.

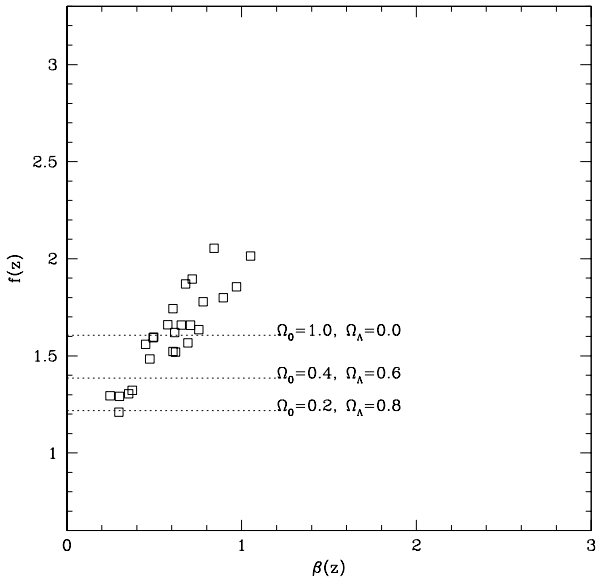

FIG. 8.—Results for fits to the same 25 realizations as in Fig. 7, reducing the noise in the correlation function across the line of sight by a factor of 2 and the noise in the line-of-sight correlation by a factor of 6. This corresponds to the use of Lyα forest spectra from 24 pairs of quasars and 384 single quasars. The horizontal dotted lines indicate the theoretical value of $f(z)$ for three cosmological models. With these large numbers of quasars, models with low density and a cosmological constant begin to be distinguishable from an Einstein–de Sitter model.

measurement of f. In Figure 9 we plot the 90% confidence level error bars in the measurement of f for $\beta = 0.2$, 0.6, and 1.0. In these cases, we fix the value of β at the assumed value in the realizations instead of allowing it to vary as in previous figures. The sets of quasars used are the same six pairs of Figure 7, so Figure 9 can be compared directly with Figure 7 to see the effect of predicting the peculiar velocity distortion. The reduction in the error of f once β is known is very substantial, allowing a cosmologically significant measurement with only six pairs. For 24 quasar pairs, and when β is known, the error bars are further reduced by a factor of 2, the 1 σ error in $f \sim \pm 10\%$.

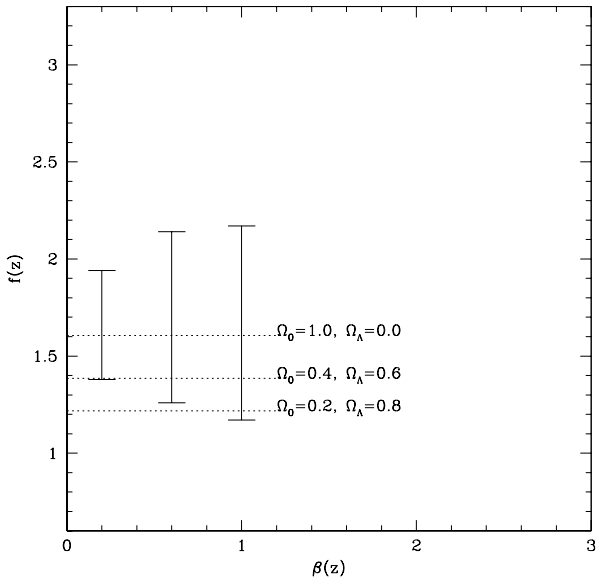

FIG. 9.—Estimate of the scatter in measuring f, assuming that the parameter β is known theoretically and the same six pairs of quasars as in Fig. 7 are available. The error bars exclude one point out of 25 realizations at each extreme, i.e., they represent approximately the 90% confidence range. The true value of f is 1.6 in the random realizations. We show $\beta = 0.2$, 0.6, and 1.0. In this case, a meaningful measure of f is already possible with six pairs of quasars.

4. DISCUSSION

We have presented a method for analyzing the Lyα forest spectra along parallel lines of sight in order to extract the geometric parameter $f(z)$ and the quantity determining the strength of peculiar velocity distortions $\beta(z) \simeq \Omega^{0.6}/b$. We have worked here in the context of the linear regime, where the correlation function is small and the peculiar velocities generally cause large-scale structures (with positive or negative density fluctuations) to be flattened along the line of sight. Using the Gaussianization technique of Croft et al. (1998), one can measure the full redshift space correlation function and obtain β and $f(z)$. Using a model in which we distribute a realistic set of discrete lines randomly in space, we have estimated the statistical errors expected for a measurement of the correlation function. To provide a useful constraint for distinguishing competing cosmological models, the value of f must be measured with an accuracy $\sim 20\%$. At least six pairs of quasars are needed to achieve that accuracy when β is known theoretically, and many more pairs are needed if β needs to be determined as well.

There are currently ~ 10 observed quasar pairs that could be suitable for this test (e.g., Fang et al. 1996; D'Odorico et al. 1998). If all of the present data were combined and the Lyα forest theory understood well enough to predict β, a cosmologically interesting measurement would be marginally possible already (see Fig. 9). A factor of a few increase in the number of pairs is needed for an accurate cosmological measurement of f and a simultaneous measurement of β. The Sloan Digital Sky Survey (SDSS) will increase the quasar database by a factor of roughly 10.[3] A systematic error-limited measurement of the cosmological geometry using the method proposed here may thus be possible in the near future, along with a detailed test of the theoretical predictions for peculiar velocity distortions in the Lyα forest.

Even though our results demonstrate that a large database will be needed to constrain the cosmological geometry from the Lyα forest correlation function in the large scales where fluctuations are in the linear regime, we expect that the parameter f should be easier to measure at smaller transverse separations in the nonlinear regime. The amplitude of the correlation function is then much larger, so many fewer pairs of quasars should be needed to measure the anisotropy of the correlation function to a fixed relative accuracy, which is required to constrain f to interesting levels. For small separations, the effect of peculiar velocities should be opposite to that in the linear regime: the correlation function should be elongated along the line of sight. This is caused by the well-known "fingers of God" effect in galaxy redshift surveys (where high-density clusters appear as highly elongated filaments pointing toward us). In the Lyα forest, the "fingers of God" effect is simply the contribution of the internal velocity dispersion (either hydrodynamic or thermal) of the absorbers to their width.

[3] The SDSS survey is described at http://www.astro.princeton.edu/BBOOK/SCIENCE/QUASARS/quasars.html.

The disadvantage of working in the nonlinear regime is that the anisotropy of the correlation function can only be predicted with numerical simulations. Therefore, we can only measure f if we can be certain that numerical simulations are accurate enough. Another important reason to measure the two-point function in the nonlinear regime is that it should provide a very powerful test of the results of numerical simulations and the large-scale structure theories in which they are based. The full redshift space two-point function gives a more quantitative test of the theory of the Lyα forest than the measurement of transverse sizes of the absorbers from coincidences of lines (Crotts & Fang 1998 and references therein).

On the large scales, an alternative to finding a large number of pairs of bright quasars to measure the anisotropy of the linear correlation function to high accuracy could be to work with spectra of much fainter but much more numerous sources. So far, observational studies of the Lyα forest have used bright quasars as sources because of the desired high resolution and signal-to-noise ratio that are necessary to measure the properties of individual absorption lines. But as we have discussed previously, the limit in the accuracy of measuring the Lyα forest correlation function on large scales is determined by the cosmic variance of the Lyα forest itself rather than the signal-to-noise ratio or resolution of the observations. Therefore, the correlation function could in principle be obtained from spectra of much poorer quality than the usual observations of bright quasars, as long as a very large number of sources are observed. Recently, large numbers of galaxies are being identified at high redshift with the method of the Lyman-limit break technique (Steidel et al. 1996). Spectra are now being taken routinely of galaxies in the redshift range 2.5–4, which have a number density of ~ 1 galaxy per square arcminute (Steidel et al. 1998). If the stellar continuum of the galaxies can be modeled, the Lyα forest spectra in these galaxies could provide a better way to measure the Lyα forest correlation on large scales along and across the line of sight. The Lyman-limit break galaxies could provide the best chance to measure the Lyα forest transverse correlation to measure the parameter $f(z)$ to high enough accuracy to constrain the cosmological geometry.

REFERENCES

Alcock, C., & Paczyński, B. 1979, Nature, 281, 358
Ballinger, W. E., Peacock, J. A., & Heavens, A. F. 1997, MNRAS, 282, 877
Bardeen, J. M., Bond, J. R., Kaiser, N., & Szalay, A. S. 1986, ApJ, 304, 15
Bechtold, J., Crotts, A. P. S., Duncan, R. C., & Fang, Y. 1994, ApJ, 437, L83
Croft, R. A. C., Weinberg, D. H., Katz, N., & Hernquist, L. 1997, ApJ, 488, 532
———. 1998, ApJ, 495, 44 (CWKH)
Crotts, A. P. S., & Fang, Y. 1998, ApJ, 502, 16
Dinshaw, N., Impey, C. D., Foltz, C. B., Weymann, R. J., & Chaffee, F. H. 1994, ApJ, 437, L87
D'Odorico, V., Cristiani, S., D'Odorico, S., Fontana, A., Giallongo, E., & Shaver, P. 1998, A&A, 339, 678
Fang, Y., Duncan, R. C., Crotts, A. P. S., & Bechtold, J. 1996, ApJ, 462, 77
Fisher, K. B. 1995, ApJ, 448, 494
Hamilton, A. J. S. 1992, ApJ, 385, L5
Hui, L. 1998, preprint (astro-ph/9807068)
Hui, L., & Gnedin, N. 1997, MNRAS, 292, 27
Kaiser, N. 1987, MNRAS, 227, 1
Kaiser, N., & Peacock, J. A. 1991, ApJ, 379, 482
Kim, T., Hu, E. M., Cowie, L. L., & Songaila, A. 1997, AJ, 114, 1
Lilje, P. B., & Efstathiou, G. 1989, MNRAS, 236, 851
Ma, C. 1996, ApJ, 471, 13
Matsubara, T., & Suto, Y. 1996, ApJ, 470, L1
Peebles, P. J. E. 1993, Principles of Physical Cosmology (Princeton: Princeton Univ.)
Rauch, M., et al. 1997, ApJ, 489, 7
Steidel, C. C., Adelberger, K. L., Dickinson, M., Giavalisco, M., Pettini, M., & Kellogg, M. 1998, ApJ, 492, 428
Steidel, C. C., Giavalisco, M., Pettini, M., Dickinson, M., & Adelberger, K. L. 1996, ApJ, 462, L17
Theuns, T., Leonard, A., Schaye, J., & Efstathiou, G. 1998, MNRAS, in press
Weinberg, D. H. 1992, MNRAS, 254, 315